

TABLE I. Experimental and theoretical quantum defects for  $s$ ,  $p$ ,  $d$ , and  $f$  waves in Rb and Xe.

Element	Angular	Experimental	Calculated
	momentum		
Rb	0	3.14	3.15
Rb	1	2.66	2.74
Rb	2	1.35	1.47
Rb	3	0.01	0.00
Xe	0	4.02	3.90
Xe	1	3.56	3.46
Xe	2	2.43	2.22
Xe	3	0.03	0.00

parison, as well as a similar comparison of other quantities calculated from HS potentials such as

the photo-ionization calculations of Ref. 4, gives an assessment of the accuracy of the HS potentials. The question can then be asked – can one replace systematically the HS by a substantially better central potential? If not, comparison of experimental phase shifts with those given in this paper provide an experimental characterization of nonlocal exchange effects.

#### IV. ACKNOWLEDGMENTS

The author would like to thank Professor Ugo Fano, for suggesting this problem and for several discussions, as well as John Cooper, Mitio Inokuti, and A. R. P. Rau for valuable suggestions and comments.

\*Present Address: Department of Physics, Georgia State College, Atlanta, Georgia 30303.

<sup>1</sup>A. R. P. Rau and U. Fano, *Phys. Rev.* **167**, 7 (1968).

<sup>2</sup>F. Herman and S. Skillman, *Atomic Structure Calculations* (Prentice-Hall, Inc., Englewood Cliffs, New Jersey, 1963).

<sup>3</sup>M. J. Seaton and G. Peach, *Proc. Phys. Soc. (London)* **79**, 1296 (1962).

<sup>4</sup>S. T. Manson and J. W. Cooper, *Phys. Rev.* **165**, 126 (1968).

<sup>5</sup>A. Messiah, *Quantum Mechanics* (North-Holland Publishing Company, Amsterdam, 1961) Vol. 1, p. 404.

<sup>6</sup>M. J. Seaton, *Compt. Rend.* **240**, 1317 (1955).

<sup>7</sup>C. E. Moore, *Atomic Energy Levels National Bureau of Standards Circular No. 467* (U.S. Government Printing Office, Washington, D. C., 1949).

## Cross Sections for Electron Capture into the Excited Level $n = 6$ of Hydrogen by 5- to 70-keV Protons in Mg Vapor and in Neon\*

Klaus H. Berkner, William S. Cooper III, Selig N. Kaplan, and Robert V. Pyle  
*Lawrence Radiation Laboratory, University of California, Berkeley, California 94720*  
 (Received 7 November 1968)

An optical technique has been used to investigate electron capture into the excited level  $n = 6$  of hydrogen by 5- to 70-keV protons passing through magnesium vapor or neon. Photons from the Balmer  $H_{\delta}$  transition which are emitted downstream of the target were analyzed with a grating spectrometer and counted. From these the population of the level  $n = 6$  and the cross section for electron capture into  $n = 6$  have been obtained. Cross-section estimates for ionization of the level  $n = 6$  collisions with Mg atoms are also presented. The electron-capture cross sections are consistent with  $n^{-3}$  extrapolations of electric-gap measurements for capture into higher quantum levels ( $n \approx 9$  to 15) reported by Il'in and co-workers, Futch and Moses, and Riviere. The results are compared with those of various theoretical models.

### I. INTRODUCTION

At proton energies between about 5 and 30 keV, cross sections for electron capture from metal

vapors are much larger than those for capture from common gases. We have investigated one particular vapor, magnesium, and report here cross-section measurements for electron capture into

the  $n=6$  level of hydrogen by 5- to 70-keV protons. To demonstrate the difference between metal vapors and other gases, we also report measurements for capture from neon. Total capture and loss cross-section measurements for magnesium have been reported in a separate paper.<sup>1</sup>

The desirability of metal vapors as charge-exchange media for the formation of excited hydrogen atoms has long been recognized in polarized-ion-source technology where metals have been used for the production of hydrogen atoms in the  $2s$  metastable state.<sup>2</sup> For some thermonuclear fusion experiments, hydrogen atoms in more highly excited states are of interest, and Hiskes and Mittleman showed theoretically that lithium and cesium should be desirable charge-exchange materials for this purpose.<sup>3</sup> This was confirmed in an experiment by Futch and Damm,<sup>4</sup> who showed that the population of the excited levels with principal quantum numbers  $n \approx 9$  to 13 was enhanced when lithium, rather than water vapor, was used as a charge-exchange medium for 35-keV  $D^+$ .

Subsequently Il'in and co-workers surveyed electron capture from metal vapors of groups I and II of the periodic table.<sup>5-7</sup> A theoretical survey of electron capture into excited states from many elements has recently been completed by Hiskes.<sup>8</sup> Magnesium, in particular, has received considerable attention: Measurements have been reported by Il'in and co-workers,<sup>5,7</sup> by Futch and Moses,<sup>9</sup> and by Riviere.<sup>10</sup> In these experiments the electric-gap technique (field ionization of highly excited states) was used to determine the populations of highly excited levels ( $n \approx 9$  to 16): It was assumed that the fractional population of a level  $n$  is given by  $\alpha n^{-3}$ , and the constant  $\alpha$  was determined experimentally. The measurements of  $\alpha$  are in reasonable agreement with theoretical estimates by Hiskes for the ratio of the cross section for capture into an excited level (comparisons are usually made for  $n=11$ ) to that for capture into all levels.

We have used an optical technique to investigate electron capture into the excited level  $n=6$  by 5- to 70-keV protons passing through Mg vapor. In the experiment photons from the Balmer  $H_\delta$  transition which are emitted downstream of the Mg target were counted. From these counts the population of the  $n=6$  level and the cross section for electron capture into  $n=6$  have been obtained. From the variation of the population of  $n=6$  with target thickness we deduce effective cross sections for excitation to and loss from  $n=6$  by collisions with Mg atoms.

Our motivation for using the optical rather than the electric-gap technique in this experiment was that (a) measurements are more easily carried out at low-proton energies and (b) excited states of the entire beam emerging from the charge-ex-

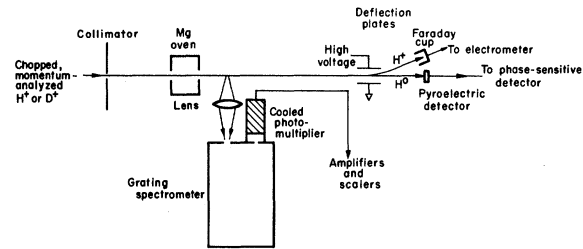


FIG. 1. Experimental arrangement.

change cell are included, thereby averaging possible variations of excitation over the angular distribution of the emerging beam. The optical technique, however, introduces complications in the interpretation of the data, as will be described later. Of the optically accessible levels, we chose  $n=6$ , because  $n$  is large enough that  $F(n)$  is proportional to  $n^{-3}$ , making comparison with other experiments simple, and it yields higher counting rates than do levels with larger quantum numbers.

## II. APPARATUS AND PROCEDURE

The experimental arrangement Fig. 1 differs from that described in Ref. 1 only by the addition of an optical system for the detection of  $H_\delta$  radiation. A collimated, momentum-analyzed beam of  $H^+$  or  $D^+$  passed through an oven in which Mg was heated to produce Mg vapor. After charge-exchange collisions in the oven, the beam contained  $H^+$ ,  $H^-$ , and  $H$  atoms in various excited states. The pressure (approximately  $10^{-6}$  Torr) in the drift region was sufficiently low that interactions with the background gas were negligible. The radiation from the decay of excited states was focused by a quartz lens onto the entrance slit of a grating monochromator which was set to analyze Balmer  $H_\delta$  radiation. The charge components were separated electrostatically and detected. In this paper we describe only the optical system, and we refer to Ref. 1 for a description of the oven, and the detection of beam particles.

The photon detection system consisted of a quartz lens, a grating spectrometer, and a photomultiplier tube. The lens focused light from a 0.48-cm-long section of the beam beginning 1.1 cm from the exit collimator of the oven onto the entrance slit of the spectrometer, which was aligned parallel to the beam axis. In this experiment sensitivity was more important than spectral resolution; consequently, we used 1.73-mm-wide entrance and exit slits on the spectrometer. This resulted in a spectral resolution of 30 Å full width at half maximum. The result of a spectral scan of the Balmer lines originating from the  $s$ ,  $p$ , and  $d$  states of the levels  $n=4$  to 9 is shown in Fig. 2. Note that all lines are clearly resolved

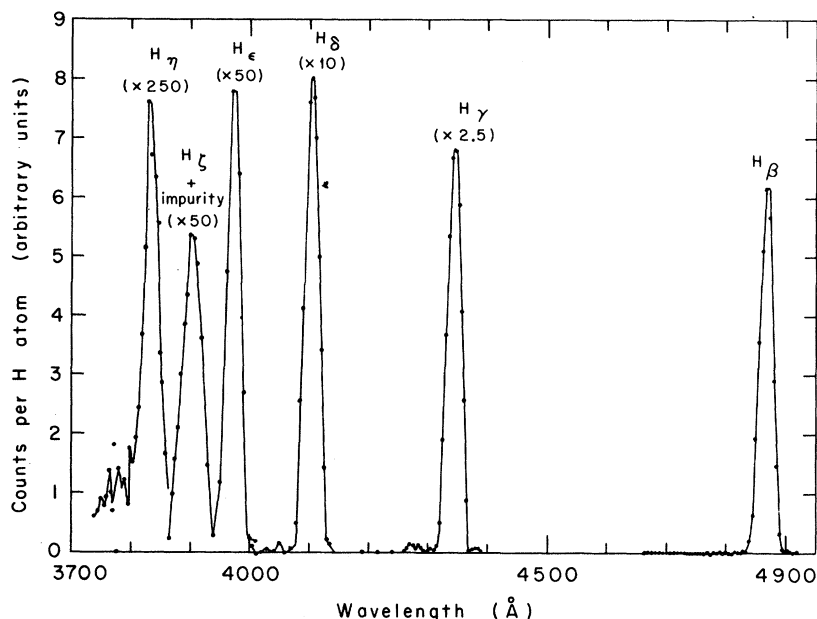


FIG. 2. Observed Balmer spectrum for 15-keV  $H^0$  produced in a magnesium-vapor target  $6.5 \times 10^{13}$ -atoms/cm<sup>2</sup> thick. No corrections for variations in spectral sensitivity have been made.

except the  $n=8$  line (3889 Å) which is broadened by an impurity line of slightly longer wavelength (probably the 3914 Å band of  $N_2^+$ ). Our study was limited to the Balmer  $H_\delta$  ( $n=6$ ) line at 4102 Å.

The system was aligned by moving the lens and scanning the beam image across the entrance slit. A sample lens scan is shown in Fig. 3; the solid line indicates the expected profile calculated by assuming that the beam is uniformly distributed in a cylinder of 1.1-mm diam, the size expected from the collimation of the incident beam. The observed profile did not change appreciably even at the highest Mg densities used, and we interpret this to mean that the beam enlargement due to scattering was negligible. The slight displacement of the oven due to thermal expansion was sufficient to displace the beam image from the center of the spectrometer entrance slit, and it was necessary to reset the lens position if the oven temperature was changed.

A photomultiplier (EMI 6256S), cooled to  $-20^\circ\text{C}$  to reduce dark current, was mounted behind the exit slit of the spectrometer. The photomultiplier signal was amplified and discriminated, and pulses arising from individual photons were counted with standard scaler circuits. Two sets of scalars were used to enable us to correct for photomultiplier noise: The incident beam was chopped at a frequency of 10.5 Hz, and one set of scalars was gated to record pulses when the beam was on, the other when the beam was off (i. e., noise pulses). The beam-off counts were subtracted from the

beam-on counts to yield the number of pulses produced by the beam.

To determine the overall detection efficiency of the optical system, we looked at the decay of excited states of  $N_2^+$  which are produced by proton bombardment of  $N_2$ . Of particular interest to us was the  $O-O$  band (3914 Å) of the first negative band system of  $N_2^+(B^2\Sigma_u \rightarrow X^2\Sigma_g)$ , since it lies very close to the Balmer  $H_\delta$  (4102 Å) line. We

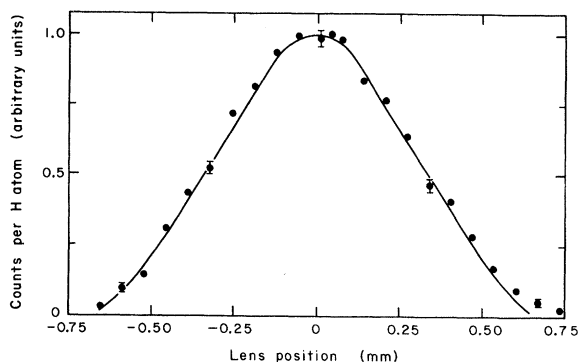


FIG. 3. Dependence of the photon signal on lens position. The solid line is the profile calculated from the lens geometry and the assumption that the beam is uniformly distributed over a 1.1-mm-diam cylinder, the size expected from beam collimation. The points are experimental results for 30-keV  $H^0$  produced in a target  $5.5 \times 10^{13}$ -Mg-atoms/cm<sup>2</sup> thick; the error bars are based on counting statistics.

TABLE I. Emission cross section measurements ( $10^{-17}$  cm<sup>2</sup>/molecule) of the  $O-O$  first negative band of  $N_2^+$  (3914 Å) produced by bombardment of  $N_2$  by 60-keV  $H^+$ .

Philpot and Hughes (1964), Ref. 11	$5.6 \pm 2.2$
Dufay, Desesquelles, Druetta, and Eidelsberg (1966), Ref. 12	$3.0 \pm 1.5$
Robinson and Gilbody (1967), Ref. 13	$3.35 \pm 0.7$
Thomas, Bent, and Edwards (1968), Ref. 14 (extrapolated from 75 keV)	$2.2 \pm 0.6$
Weighted average	$2.8 \pm 0.4$

estimate that the detection efficiency of our system varies by less than 5% between 3914 and 4102 Å. Measurements of the emission cross sections for this band have been reported by several groups,<sup>11-14</sup> and in Table I we list their results and quoted uncertainties for impact by 60-keV protons. The experimental procedure was to admit  $N_2$  gas to the region viewed by the lens, adjust the proton energy to 60 keV, and set the spectrometer to observe the 3914 Å band.<sup>15,16</sup> A plot of counts per incident proton versus pressure was quite linear over the pressure range used,  $2 \times 10^{-6}$  to  $1 \times 10^{-4}$  Torr. The pressure was measured with a capacitance manometer and an ionization gauge. From the slope of this curve and the length of the beam path viewed by our system, we obtained a number which is the product of the emission cross section and the detection efficiency. Using a weighted average of the emission cross sections listed in Table I, we find the overall detection efficiency of our optical system to be  $(8.5 \pm 1.6) \times 10^{-5}$  at 4102 Å; the uncertainty is due mainly to uncertainty in the value of the emission cross section. This *in situ* determination was repeated periodically; except for day-to-day scatter of  $\pm 5\%$ , we observed no change in the efficiency over a period of three months.

The calculation of the overall detection efficiency is more complicated if the 3914 Å  $N_2^+$  band and the  $H\delta$  line have different polarizations and the sensitivity of the detecting system depends on the polarization. We used a Polaroid polarizing filter and an incandescent lamp behind a piece of ground glass to determine the relative sensitivity of the detection system for polarizations parallel to and perpendicular to the beam direction. We then measured the polarization of the 3914 Å  $N_2^+$  calibration band at 60 keV and found it to be  $-2 \pm 3\%$ , consistent with measurements reported in Ref. 14. The polarization of the  $H\delta$  line resulting from electron capture in a thin Mg target was measured at 15 and 30 keV and was found to be  $4 \pm 3\%$ . Since these measurements indicated that the  $N_2^+$  band and the  $H\delta$  line are both essentially unpolarized, no polarization correction was necessary in calculating the detection efficiency.

If the radiation from the beam is isotropic, the number of  $H\delta$  photons emitted in the observation region is related directly to the number of observed pulses by the inverse of the detection efficiency. The radiation pattern for a polarized line is not isotropic, but the deviation from isotropy can readily be calculated in terms of the angle of observation and the polarization of the light radiated perpendicular to the beam.<sup>17</sup> For our measured polarization this deviation is less than 2%; since this is negligible compared to other experimental uncertainties it has been neglected.

The number of counts from radiation at 4102 Å and the integrated signal from the H detector were measured simultaneously. This was done both with the electrostatic analyzer on, in which case the H detector measured the neutral component, and with the analyzer off, in which case the detector measured the total incident beam. From these measurements and the various calibration factors, we obtained the number of photons emitted in the observation region per H atom, the number of photons emitted per incident proton, and the number of H atoms per incident proton (neutral fraction  $F_0$ ). The variation of these three quantities with target thickness  $\pi$  (atoms/cm<sup>2</sup>) is illustrated in Figs. 4 and 5. The solid lines shown in these figures are discussed in Sec. IV B.

### III. DATA ANALYSIS

To relate the photon signal to the population of the  $n=6$  level in the oven, we must make assumptions about the population distribution over the various substates of  $n=6$ , and the appropriate transition probabilities. We will assume that (a)

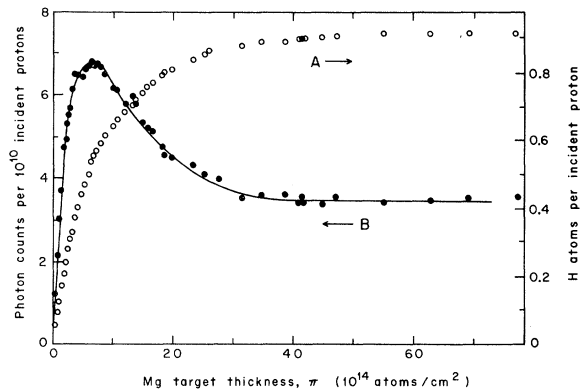


FIG. 4. Dependence of the neutral fraction  $F_0$  on Mg-target-thickness  $\pi$  (curve A) and the number of  $H\delta$  photon counts per incident proton versus target thickness (curve B). The beam energy was 15 keV. The curve is the result of a least-squares fit to the solution of a three-level model with two adjustable parameters: (a) the cross sections for excitation from the ground state and (b) ionization of the level  $n=6$  (see discussion in Sec. IVB).

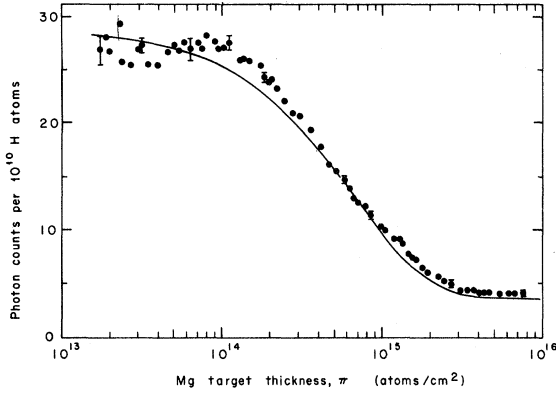


FIG. 5. The number of  $H_{\delta}$  photon counts per H atom versus Mg-target-thickness  $\pi$ . The curve is the solution to a three-level model, using the results of the least-squares fit to the data in curve B of Fig. 4 (see discussion in Sec. IVB).

the population within the oven has a statistical distribution over substates, (b) outside of the oven there is no mixing among states, and (c) the states decay with field-free lifetimes. These assumptions will be discussed later in this section.

In this model the number of atoms within the oven in a substate  $6l$  is  $(2l+1)N_6^0/36$ , where  $N_6^0$  is the total number of atoms in the  $n=6$  level. The transition probabilities, decay lengths, and velocities in our experiment are such that exponentials can always be approximated to better than 5% by a linear expansion; therefore, we can average over the length of the oven by considering all excited atoms to be formed at the center of the oven and decaying with the statistically averaged transition probability

$$A(6l) = \sum_{l'=0}^5 \sum_{n'} \frac{(2l+1)}{36} A(6l \rightarrow n'l'), \quad (1)$$

where  $n'$  and  $l'$  denote all lower states that can be reached by radiative transitions. Once the atoms leave the oven there is no longer any shuffling between states, and each state decays with a transition probability

$$A(6l) = \sum_{l', n'} A(6l \rightarrow n'l'). \quad (2)$$

Only three transitions ( $6s \rightarrow 2p$ ,  $6p \rightarrow 2s$ , and  $6d \rightarrow 2p$ ) contribute to Balmer  $H_{\delta}$  radiation. Thus in the observation region only a fraction  $A(6l \rightarrow 2s, p)/A(6l)$  of the transitions contribute to the  $H_{\delta}$  signal. Neglecting cascade contributions to the population of  $n=6$ ,<sup>18</sup> we can express the number of  $H_{\delta}$  photons emitted in the observation region as

$$N(H_{\delta}) = N_6^0 \exp[-v^{-1}x_1 A(6)] \\ \times \sum_{l=0}^2 \frac{2l+1}{36} \exp[-v^{-1}x_2 A(6l)] \\ \times \frac{A(6l \rightarrow 2s, p)}{A(6l)} \{1 - \exp[-v^{-1}x_3 A(6l)]\}, \quad (3)$$

where  $x_1$  is the distance from the midpoint to the exit of the oven,  $x_2$  is the distance from the oven exit to the observation region,  $x_3$  is the length of the observation region, and  $v$  is the velocity of the atoms. To evaluate the expression we used transition probabilities calculated by Hiskes and Tarter<sup>19,20</sup> (see Table II). The distances  $x_1$ ,  $x_2$ , and  $x_3$  were 2.2, 1.1, and 0.48 cm for our experimental configuration. Although the values of  $N(H_{\delta})$  presented later were obtained from Eq. (3), a simple expression, accurate to 4% in our energy range, is obtained if we expand all exponents to first order and rewrite Eq. (3) in terms of the energy of the atoms expressed in keV:

$$N_6^0 = 10^3 N(H_{\delta}) (11/E^{1/2} - 6.1/E)^{-1}. \quad (4)$$

We conclude this section with a brief comment on the assumptions used in our analysis. Our derived capture cross sections depend in a rather complicated way on the distribution over substates of the  $n=6$  level and the radiative transition rates of the substates. Both of these quantities may be affected by electric fields. Aside from the small stray electric fields that may exist in our apparatus, the atoms experience an electric field  $\vec{E} = \vec{v} \times \vec{B} \leq 2$  V/cm due to motion across the earth's magnetic field.

The Born-approximation calculations by Hiskes show that in the absence of an external electric field, essentially all of the capture is into the  $s$ ,  $p$ , and  $d$  states. If the capture occurs in a sufficiently strong electric field, the fraction of the excited states that would be in the  $d$  state, for example, is distributed over five Stark states (see the Appendix) in a way that has not been calculated yet. After the neutral atom is formed in the  $n=6$  level, shuffling among the substates may occur because of collisions with target atoms or Stark mixing in spatially varying electric fields. As a result there should be a diffusion through the substates tending toward a statistical distribution.

We have chosen to analyze our data with the assumptions that field-free lifetimes are applicable, and the distribution over the substates of the  $n=6$  level is statistical within the oven. Of course an exact analysis is impossible, because the populations of the substates are unknown, and the small electric fields probably make Stark decay rates appropriate for some substates and field-free rates for others. We showed that our assumptions

TABLE II. Transition probabilities ( $10^8 \text{ sec}^{-1}$ ) used in the analysis (from Ref. 19).

$A(6s \rightarrow 2p) = 0.00735$	$A(6s) = 0.0187$	$A(6) = 0.0519$
$A(6p \rightarrow 2s) = 0.0286$	$A(6p) = 0.245$	
$A(6d \rightarrow 2p) = 0.0514$	$A(6d) = 0.0839$	

are not precisely correct at proton energies of 30 and 60 keV by applying transverse magnetic fields of up to 20 G in the oven and observation regions. The equivalent electric fields were sufficient to ensure Stark lifetimes,<sup>21</sup> and in our model should have made the photon counting rate rise slightly (see Appendix). Experimentally the counting rates dropped  $(20 \pm 10)\%$ .<sup>22-26</sup>

The effects of making some different assumptions about substate distributions are given in the Appendix. We note that it is unlikely that the calculated cross sections shown in Figs. 6 through 10 could be increased appreciably by any other reasonable set of assumptions. However, if it should be shown that capture takes place as calculated by Hiskes, and that shuffling among substates is an unlikely process, then our calculated cross sections would be reduced by factors of roughly 2 to 3.

#### IV. RESULTS FOR A MAGNESIUM TARGET

##### A. Cross Sections for Electron Capture into $n = 6$

By using Eq. (4) we can now relate the number of photons emitted in  $x_3$  to the population of the

TABLE III. Cross sections for electron capture into the level  $n = 6$  from Mg, expressed in  $\text{cm}^2/\text{atom}$  and as a fraction  $R(6)$  of the total capture cross section  $\sigma_{10}$ , which was taken from Ref. 1. The indicated standard errors do not include possible systematic errors estimated to be  $\pm 30\%$  for the cross section and  $\pm 20\%$  for the ratio (Sec. IVA).

Proton Energy (keV)	$\sigma[\text{H}^+ \rightarrow \text{H}(n=6)]$ ( $10^{-18} \text{ cm}^2/\text{atom}$ )	$R(6)$
5	$3.6 \pm 1.1$	$0.0024 \pm 0.0008$
7.5	$8.0 \pm 1.6$	$0.0036 \pm 0.0009$
10	$8.7 \pm 1.6$	$0.0056 \pm 0.0013$
15	$14.4 \pm 2.2$	$0.0135 \pm 0.0029$
20	$10.5 \pm 1.8$	$0.0170 \pm 0.0039$
25	$6.0 \pm 0.7$	$0.0152 \pm 0.0029$
30	$3.9 \pm 0.5$	$0.0173 \pm 0.0034$
35	$2.6 \pm 0.2$	$0.0183 \pm 0.0045$
40	$1.5 \pm 0.2$	$0.0180 \pm 0.0038$
50	$0.48 \pm 0.07$	$0.0118 \pm 0.0025$
60	$0.25 \pm 0.17$	$0.0090 \pm 0.0063$
70	$0.15 \pm 0.08$	$0.0070 \pm 0.0039$

level  $n = 6$  in the target, and from the linear dependence of the photon signal on  $\pi$  at low pressures (Fig. 4) we can obtain a cross section for electron capture into the  $n = 6$  level,  $\sigma[\text{H}^+ \rightarrow \text{H}(n = 6)]$ . The results are presented in Table III. The standard errors given in the table are our estimates of the relative reliability of the cross sections. To obtain an absolute uncertainty for the cross sections, we must also fold in a standard error of  $\pm 30\%$  resulting from two possible sources of systematic error, the determination of the photon detection efficiency discussed in Sec. II ( $\pm 20\%$ ) and the determination of the Mg vapor pressure ( $\pm 20\%$ ) discussed in Ref. 1. We are not able to assign an uncertainty to the cross sections resulting from our assumption of a statistical substate distribution in the oven (Sec. III).

In Fig. 6 we compare our results with an  $n^{-3}$  extrapolation of the measurements by Il'in *et al.*<sup>5</sup> for capture into the levels  $n = 9$  to 16. Also shown in Fig. 6 are the results of various theoretical

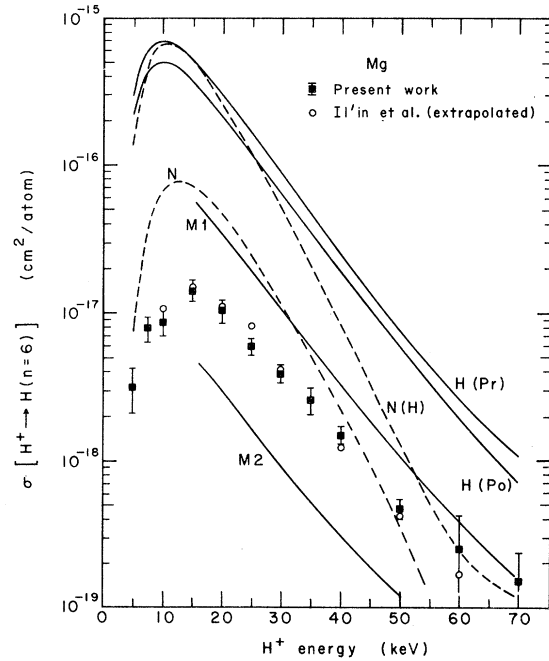


FIG. 6. Cross section for electron capture into the level  $n = 6$  for the process  $\text{H}^+ + \text{Mg} \rightarrow \text{H}(n=6) + \dots$  versus proton energy. Experimental:  $\blacksquare$ , present work;  $\circ$ , Ref. 5. Theoretical: H(Pr) and H(Po) are Brinkman-Kramers (B-K) prior and post calculations by Hiskes; N(H) is a B-K calculation by Hiskes using hydrogen-like wave functions (see Sec. IVA). Curve N was obtained by adjusting N(H) with Nikolaev's semi-empirical prescription of Ref. 30; curve M1 was obtained by multiplying the average of H(Pr) and H(Po) by ratios suggested by Mapleton, Refs. 28 and 29; curve M2 was obtained by adjusting Hiskes's B-K cross sections for capture into the *ground* state following a suggestion by Mapleton (see Sec. IVA).

models for the capture cross sections, all based on the Brinkman-Kramers (B-K) form of the first Born approximation.<sup>27</sup> Although the B-K results are known to overestimate the capture cross sections at low energies, such calculations have been useful in describing electron capture: Hiskes has shown that *ratios* of cross sections calculated in the B-K approximation are in reasonable agreement with measurements.<sup>8</sup> Alternatively, Mapleton<sup>28, 29</sup> and Nikolaev<sup>30</sup> have determined correction factors with which to adjust B-K cross sections; for total electron capture from the common gases these approaches have been quite successful.

For the determination of cross-section ratios Hiskes has calculated B-K cross sections for electron capture into individual quantum states ( $n=1$  to 11) for many of the elements. His results for capture of the  $3s^2$ ,  $2p^6$ , and  $2s^2$  electrons of magnesium into the level  $n=6$ , using the best available wave functions<sup>31</sup> in the prior and post approximations, are given by curves H(Pr) and H(Po) in Fig. 6.<sup>32</sup>

Nikolaev<sup>30</sup> has determined an empirical expression with which to adjust B-K cross sections calculated with the post-interaction and hydrogen-like wave functions with  $Z = Z_{\text{eff}}/n_{\text{eff}}$  determined by Slater's method.<sup>33</sup> To allow comparison with the present experimental results, Hiskes has evaluated this form of the B-K cross section [curve N(H)],<sup>32</sup> and we have applied Nikolaev's expression to curve N(H) to obtain curve N.

A different scaling procedure for Brinkman-Kramers cross sections has been used by Mapleton.<sup>28</sup> Cross sections for electron capture from hydrogen calculated in the Jackson-Schiff (J-S) form of the first Born approximation<sup>27</sup> agree quite well with measurements, and Mapleton has shown that good agreement with experiment is obtained for nitrogen, oxygen, and argon if the (J-S)/(B-K) ratio, evaluated for capture into H(1s) from hydrogen, is used to adjust the B-K results for the target of interest.<sup>29</sup> Although this method of scaling B-K results has been proposed for, and applied to, *total* capture cross sections, we have used these ratios to adjust Hiskes's B-K results for capture into  $n=6$ . Curve M1 is the result of multiplying the average of curves H(Pr) and H(Po) by the (J-S)/(B-K) ratios.

As an alternative, Mapleton has suggested that one might be able to estimate capture into an *excited* level of hydrogen by applying the following scaling procedure to B-K cross sections for capture into the *ground* state<sup>34</sup>: First multiply the B-K results by the (J-S)/(B-K) ratio to obtain the cross section for capture into H(1s). Then, to obtain the cross section for capture into a level  $n$ , multiply this result by the ratio

$$R(n) = |F_{100}(\vec{A}_f)|^{-2} \sum_{l=0}^{n-1} \sum_{m=-l}^l |F_{nlm}(\vec{A}_f)|^2,$$

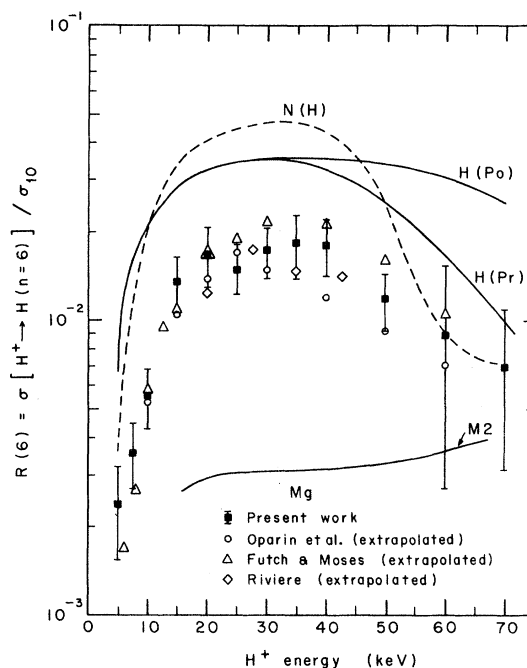


FIG. 7. Cross section for electron capture from Mg into the  $n=6$  level, expressed as a fraction of the *total* electron capture cross section  $\sigma_{10}$  versus proton energy. Experimental: ■, present work and Ref. 1; ○, Ref. 7; △, Ref. 9; ◇, Ref. 10 (the extrapolation procedure is described in Sec. IVA). The notation on the theoretical curves is the same as that used for Fig. 6.

where  $F_{nlm}$  is the momentum representation of the hydrogen-like wave functions describing the captured electron,<sup>35, 30</sup> and  $\vec{A}_f$  is the momentum change vector associated with the relative coordinates of the outgoing H atom.<sup>36</sup> We have evaluated the ratio  $R(6)$  for Mg and have applied this scaling procedure to the average of Hiskes's post and prior B-K results for capture into the ground state. The resulting cross section is shown as curve M2 in Fig. 6.

Our results, expressed as a ratio of capture into  $n=6$  relative to total capture,<sup>37</sup> are given in the last column of Table III and in Fig. 7. Also shown are extrapolations of experimental results by Oparin *et al.*,<sup>7</sup> Futch and Moses,<sup>9</sup> and Riviere.<sup>10</sup> In these three sets of measurements, it was assumed that the population of a level  $n$  is given by  $\alpha n^{-3}$ , and the constant  $\alpha$  was determined from field ionization of the levels  $n \approx 9$  to 16. For comparison with our  $n=6$  results we have used the reported thin-target values of  $\alpha$  and evaluated  $\alpha n^{-3}$  for  $n=6$ . The theoretical curves shown in Fig. 7 are results of the various models described previously. The Nikolaev correction is the same for all states, hence the curve previously described by N is identical to N(H). Similarly the corrections used to obtain curve M1 of Fig. 6 are independent of quantum number; consequently

TABLE IV. Cross-section estimates for magnesium target (Sec. IVB) in units of  $10^{-16}$  cm<sup>2</sup>/atom.

Proton energy (keV)	Three-level analysis		Two-level analysis	
	Excitation to $n=6$ from lower levels	Ionization <sup>a</sup> of $n=6$	Ionization <sup>b</sup> of $n=6$	Ionization <sup>c</sup> of $9 \leq n \leq 16$
10	0.0051	17	6.6	
15	0.033	31	8.0	$\geq 13$
30	0.029	15	8.3	10
50	0.032	15	9.4	
60				5

<sup>a</sup>Upper limit for  $\sigma[\text{H}(n=6) \rightarrow \text{H}^+]$  (see Sec. IVB).

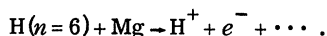
<sup>b</sup>Lower limit for  $\sigma[\text{H}(n=6) \rightarrow \text{H}^+]$  (see Sec. IVB).

<sup>c</sup>Estimates of Oparin *et al.* (Ref. 7).

curve M1 would be the average of H(Pr) and H(Po).

#### B. Estimates for Electron Loss from $n=6$

In this experiment we were not able to measure the cross section  $\sigma[\text{H}(n=6) \rightarrow \text{H}^+]$  for the process for the protons and the level  $n$ . This is the solution to a two-level system composed of protons and the level  $n$ . Because excitation to  $n$  from



However, we can estimate this cross section by analyzing the variation of the population of  $n=6$  with target thickness (Fig. 4) in terms of a three-level model in which we consider an "effective ground state,"<sup>38</sup> the  $n=6$  level, and protons.<sup>39, 40</sup> Of the five cross sections needed for the analysis described in Ref. 40 three are known: The total capture and loss cross sections (see Ref. 1) and the cross section for capture into  $n=6$ . We determined the other two cross sections, those for excitation to  $n=6$  from the lower levels and ionization of the  $n=6$  level, by a least-squares fit of our data (Fig. 4) to the solution of the three-level model. The result of such a fit is shown as the solid curve in Fig. 4. As a self-consistency check, we used these cross sections and this model to calculate the fraction of all H atoms in the level  $n=6$ ; the result is the solid line shown in Fig. 5.

The cross sections obtained in this way are given in Table IV; the quoted uncertainties indicate the effect of the standard errors of the three known cross sections. The physical interpretation for the excitation cross section obtained in this way is ambiguous because the "effective ground state" includes several levels.<sup>38</sup> The calculated "ionization cross section" characterizes the loss from  $n=6$ ; since some of the loss may be by excitation or deexcitation collisions, this should be an upper limit on the true ionization cross section for the level  $n=6$ .

A different method has been used by Oparin *et*

*al.* for estimating the ionization cross section for a level  $n$ .<sup>7</sup> They neglected excitation and calculated the ionization cross section from the relation

$$\sigma[\text{H}(n) \rightarrow \text{H}^+] = \sigma[\text{H}^+ \rightarrow \text{H}(n)] F_+^\infty / F_n^\infty,$$

where  $F_+^\infty$  and  $F_n^\infty$  are the equilibrium fractions lower levels is neglected, this analysis should give a lower limit on the ionization cross section. Applying this analysis to our results, we obtain the numbers listed in column 4 of Table IV. In column 5 we list the estimates of Oparin *et al.*<sup>7</sup> for ionization of a highly excited level.<sup>41</sup>

#### V. RESULTS FOR A NEON TARGET

We have also measured the cross section for electron capture into  $n=6$  from neon. The equipment and procedure were identical to the measurements with Mg, except that the oven was not heated and Ne was introduced through a gas line; the pressure was measured with a capacitance manometer.

The results for the total capture cross section  $\sigma_{10}$ , the cross section for capture into  $n=6$ ,  $\sigma[\text{H}^+ \rightarrow \text{H}(n=6)]$ , and the ratio  $\sigma[\text{H}^+ \rightarrow \text{H}(n=6)]/\sigma_{10}$  are given in Table V. The standard errors shown are our estimates of the uncertainty, excluding any

TABLE V. Experimental results for a neon target. The estimated standard errors in  $\sigma[\text{H}^+ \rightarrow \text{H}(n=6)]$  and  $R(6)$  do not include a possible systematic error of  $\pm 20\%$ , arising from the determination of the photon detection efficiency (Sec. II).

Proton energy (keV)	$\sigma_{10}$ ( $10^{-16}$ cm <sup>2</sup> /atom) ( $\pm 10\%$ )	$\sigma[\text{H}^+ \rightarrow \text{H}(n=6)]$ ( $10^{-19}$ cm <sup>2</sup> /atom) ( $\pm 15\%$ )	$R(6)$ ( $\pm 25\%$ )
15	2.56	2.38	0.00093
30	1.67	3.22	0.0019
45	1.15	4.52	0.0039
50	1.12	4.26	0.0038
60	0.98	3.92	0.0040



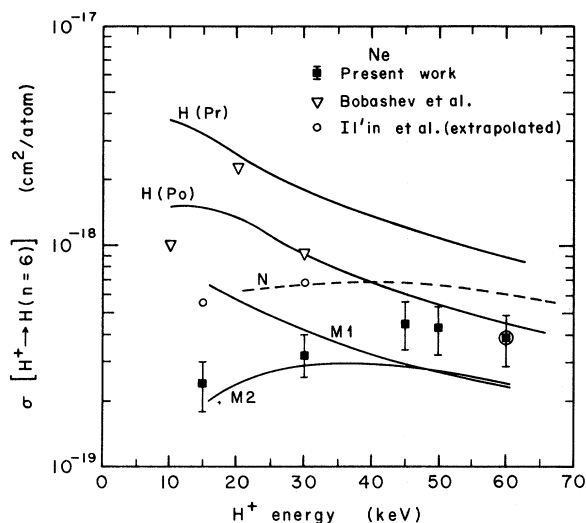


FIG. 8. Cross section for electron capture into the level  $n=6$  for the process  $H^+ + Ne \rightarrow H(n=6) + \dots$  versus proton energy. Experimental:  $\blacksquare$ , present work;  $\circ$ , Ref. 6;  $\nabla$ , Ref. 43. The notation on the theoretical curves is the same as that for Fig. 6, with the exception of curve N, which in this case was taken directly from Ref. 30.

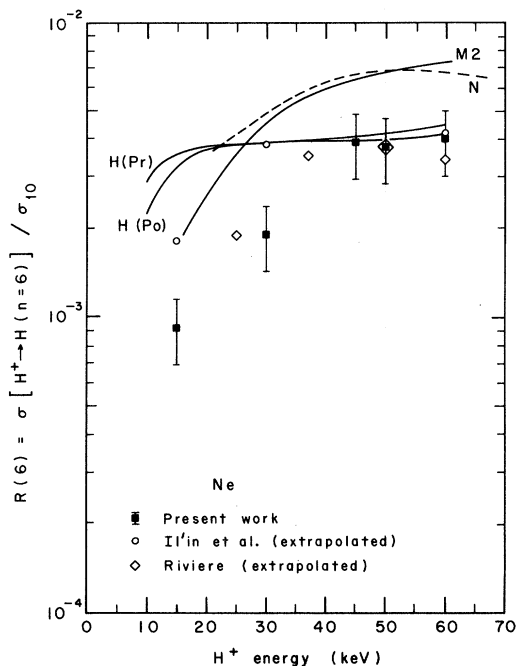


FIG. 9. Cross section for electron capture from Ne into the  $n=6$  level, expressed as a fraction of the total electron capture cross section  $\sigma_{10}$  versus proton energy. Experimental:  $\blacksquare$ , present work;  $\circ$ , Ref. 6;  $\diamond$ , Ref. 39 (the extrapolation procedure is described in Sec. IV A). The notation on the theoretical curves is the same as that for Fig. 6, with the exception of curve N, which in this case was taken directly from Ref. 30.

errors introduced by our assumption of a statistical substate distribution. The  $\sigma_{10}$  results are in excellent agreement with measurements by Stier and Barnett.<sup>42</sup>

In Figs. 8 and 9 we compare our results for capture into  $n=6$  with theoretical calculations discussed in the preceding section and with experimental results (extrapolated from higher  $n$  values) of Il'in and coworkers<sup>6</sup> and of Riviere.<sup>39</sup> Also shown are the cross sections reported by Bobashev *et al.*<sup>43</sup>; in this experiment the intensity of the Balmer  $H_{\delta}$  line was used to study electron capture in a strong magnetic field. For neon the curve N was taken directly from Ref. 30, and the intermediate B-K result N(H) was not calculated separately.

To illustrate the difference between Mg and Ne for the production of excited states, we show the ratio of  $\sigma[H^+ \rightarrow H(n=6)]$  for Mg to that for Ne in Fig. 10. Again we compare with the various theoretical results and other experiments.

## VI. DISCUSSION AND CONCLUSIONS

In a previous paper<sup>1</sup> it was shown that in the energy range where they overlap, our total capture cross-section measurements for magnesium vapor are in reasonably good agreement with measurements by others. In the present paper we note that our total cross sections for protons in neon are in good agreement with the values of Stier and

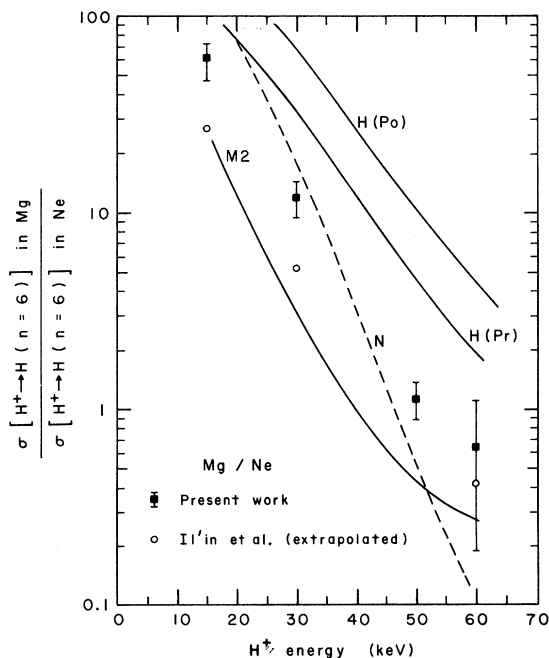


FIG. 10. Cross section for electron capture from Mg into the level  $n=6$  relative to that for capture from Ne. Experimental:  $\blacksquare$ , present work;  $\circ$ , Ref. 6. The notation on the theoretical curves is the same as that for Fig. 6.

Barnett.<sup>42</sup>

Comparisons of our excited-state yields with other experiments are more difficult. Except for the measurements in Ne by Bobashev *et al.*, other experimenters have used the electric-gap technique and, assuming an  $n^{-3}$  dependence, have deduced cross sections for hydrogen in the excited levels  $n \approx 9$  to 16.

Hiskes's calculations show that the partial capture cross sections in Mg are proportional to  $n^{-3}$  for  $n \geq 6$  at proton energies above about 10 keV and deviate from the  $n^{-3}$  extrapolation by only 15% for  $n=6$  at 5 keV. In Ne, capture into  $n \geq 6$  is quite accurately proportional to  $n^{-3}$  in the Brinkman-Kramers approximation, even at a proton energy of 5 keV. Consequently it seems reasonable to use  $n^{-3}$  extrapolations for comparison of our experimental results with those for higher  $n$  values. In Figs. 6 and 8 we show measurements by others extrapolated down to  $n=6$  and indeed find quite good agreement with the results of our measurements.

In obtaining our cross sections, however, we made an assumption about the distribution over substates of the  $n=6$  level, namely that in the oven the substates were populated according to their statistical weights. We also assumed that field-free transition probabilities can be used. If one accepts the validity of the  $n^{-3}$  dependence, the quite good agreement with extrapolations of the electric-gap measurements gives considerable confidence in the usefulness of the model. However, we emphasize that the substate distributions and the degree to which small electric fields affect the results are unknown. (Even the exponent in the  $n^{-3}$  dependence has not been verified experimentally to better than perhaps 15%. Our present measurements do not permit a check of this dependence.)

Data of the kind shown in Figs. 4 and 5 but in regions of larger  $n$  have been reported by others for several gases<sup>39</sup> and for magnesium.<sup>5,9</sup> The decrease in the fraction of the atoms in the  $n=6$  excited levels, as the gas target becomes thicker, is of course connected with a large ionization cross section for highly excited atoms. Riviere<sup>39</sup> has shown that ionization cross sections extracted from such data for the common gases are consistent with the total scattering cross section of an electron with the same speed as the atom. However, we do not know of electron-scattering data that would make such a comparison possible for magnesium. We have estimated upper and lower limits for the ionization cross section of the  $n=6$  level; our lower limits agree with those obtained in the same way by Oparin *et al.*<sup>7</sup> for the levels  $n=9$  to 16.

Opinions about comparisons between calculations and experiment are best formed by the reader after an examination of the figures. Briefly,

Hiskes's assumption that reasonable *ratios* of various quantities should be obtained from Brinkman-Kramers approximation calculations is fairly well born out for Mg and Ne, and in fact, Hiskes has shown that this is true for all cases where experimental evidence exists. (In the absence of other information one would probably average the post and prior calculations. However, Hiskes has shown that better agreement with experiment is obtained with the prior approximation alone.) Ratios obtained from the type of B-K formulation used by Nikolaev or by Mapleton's M1 prescription are also in fair agreement with experiment. A similar remark can be made about absolute cross sections for capture into an excited state, as estimated by the semiempirical formulation by Nikolaev or the semitheoretical suggestions by Mapleton.

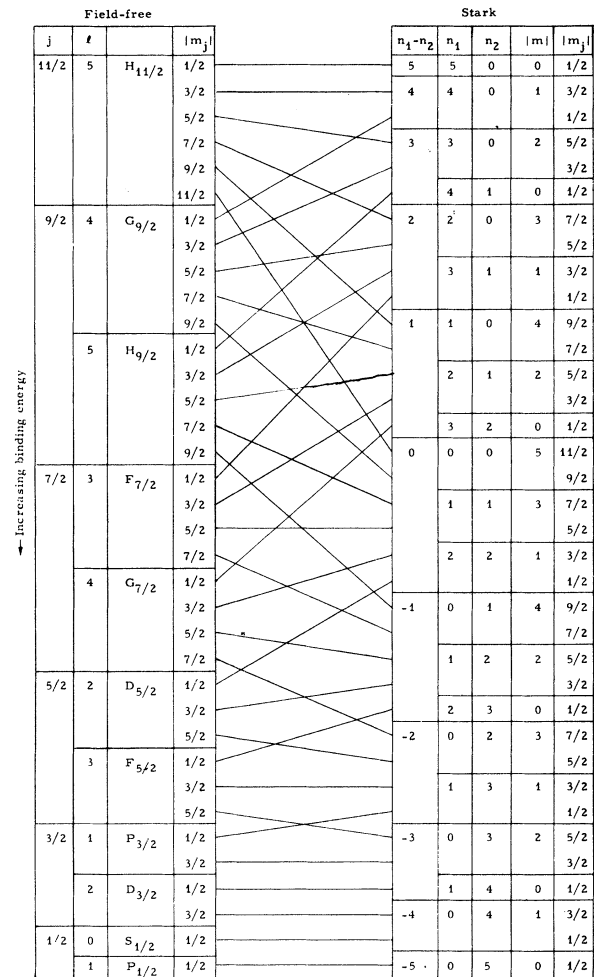


FIG. 11. Labelling of substates of the  $n=6$  level for field-free and linear Stark conditions.<sup>44</sup>

TABLE VI.  $N(\text{H}_\delta)/N_6^0$ : The fraction ( $\times 10^3$ ) of atoms captured from Mg into the  $n=6$  level that emit detectable photons with the present experimental arrangement, evaluated for several assumptions about the decay mode and the population distribution.

Assumed initial substate populations	Proton energy (keV)	Field-free lifetimes			Stark lifetimes		
		No substate shuffling	Statistical only in oven	Always statistical	No substate shuffling	Statistical only in oven	Always statistical
Statistical Hiskes-Born <sup>c</sup> <i>s</i> only <i>p</i> only <i>d</i> only	5	3.16	3.61 <sup>a</sup>	3.96	3.69	3.85	3.96
		8.63			5.54 <sup>b</sup>		
		3.37			8.16 <sup>b</sup>		
		5.78			5.79 <sup>b</sup>		
		18.6			4.00 <sup>b</sup>		
Statistical Hiskes-Born <sup>c</sup> <i>s</i> only <i>p</i> only <i>d</i> only	30	1.64	1.74 <sup>a</sup>	1.80	1.75	1.78	1.80
		5.00			2.66 <sup>b</sup>		
		1.43			3.98 <sup>b</sup>		
		3.98			2.89 <sup>b</sup>		
		9.10			1.88 <sup>b</sup>		
Statistical Hiskes-Born <sup>c</sup> <i>s</i> only <i>p</i> only <i>d</i> only	60	1.22	1.27 <sup>a</sup>	1.31	1.28	1.29	1.31
		3.23			2.16 <sup>b</sup>		
		1.02			2.92 <sup>b</sup>		
		3.13			2.13 <sup>b</sup>		
		6.67			1.37 <sup>b</sup>		

<sup>a</sup>These values are shown in Figs. 6 to 10.

<sup>b</sup>Assuming that the populations of the corresponding field-free states are uniformly distributed over the Stark states (see Fig. 11).

<sup>c</sup>Populations calculated by Hiskes, using the first Born approximation (Ref. 32). The fractional populations of the *s*, *p*, and *d* states are, respectively, 5 keV: 0.123, 0.581, 0.261; 30 keV: 0.101, 0.572, 0.283; 60 keV: 0.230, 0.576, 0.178.

#### ACKNOWLEDGMENTS

We take pleasure in thanking Dr. C. M. Van Atta for his support of this research, Dr. J. R. Hiskes for theoretical advice and for performing the Brinkman-Kramers calculations, and Dr. R. A. Mapleton for his suggestions on scaling procedures. One of us (SNK) would also like to express his appreciation to Professor B. J. Moyer and Professor A. C. Helmholtz for their support during the course of this work. Much valuable assistance was extended in the assembly and operation of equipment by J. Warren Stearns and Vincent J. Honey.

#### APPENDIX

In Table VI we give examples for three different proton energies of the calculated fractions of atoms formed in the  $n=6$  level that emit detectable  $\text{H}_\delta$  photons. The derived electron-capture cross sections are inversely proportional to the tabulated numbers. The values used in deriving the cross sections shown in Figs. 6 to 10 are designated by the superscript "a" in the table. They are based on the assumption that a statistical distribution over substates is maintained in the oven, and no

mixing occurs outside of the oven. We note that in this case the results change by only a small amount if we use Stark instead of field-free lifetimes.

Another plausible assumption is that capture takes place as calculated by Hiskes, with no subsequent shuffling among substates. This assumption leads to cross sections roughly one-half to one-third those shown in Figs. 6 to 10. Capture and decay in a sufficiently strong electric field are best described in terms of Stark substates, and the *s*, *p*, *d* substate descriptions are replaced by parabolic quantum numbers, as shown in Fig. 11.<sup>44</sup> The cross sections for electron capture into a given substate have not been calculated yet; in making up Table VI we have assumed that the calculated capture into an *s*, *p*, or *d* state is evenly distributed over the accessible Stark states.

According to Hiskes's calculations, most of the capture is into *s*, *p*, or *d* states, with essentially nothing into the *f* or higher states. As an indication that the true cross sections are not likely to be larger than those plotted in Figs. 6 to 10, we give the values of  $N(\text{H}_\delta)/N_6^0$  that would be obtained if all of the atoms were in one of the *s*, *p*, or *d* states (or the equivalent Stark states).

\*This work was done under the auspices of the U. S. Atomic Energy Commission.

<sup>1</sup>K. H. Berkner, R. V. Pyle, and J. W. Stearns, *Phys. Rev.* **178**, 248 (1969).

<sup>2</sup>See, for example, the review article by W. Haerberli in *Ann. Rev. Nucl. Sci.* **17**, 373 (1965).

<sup>3</sup>J. R. Hiskes and M. H. Mittleman, University of California Radiation Laboratory Report No. UCRL-9969, 1961 (unpublished), p. 128.

<sup>4</sup>A. H. Futch, Jr. and C. C. Damm, *Nucl. Fusion* **3**, 124 (1963).

<sup>5</sup>R. N. Il'in, V. A. Oparin, E. S. Solov'ev, and N. V. Fedorenko, in *Proceedings of the Fourth International Conference on the Physics of Electronic and Atomic Collisions, Quebec, 1965* (Science Bookcrafters, Inc., New York, 1965); R. N. Il'in, V. A. Oparin, E. S. Solov'ev, and N. V. Fedorenko, *Zh. Eksperim. i Teor. Fiz., Pis'ma Redakt.* **2**, 310 (1965) [English transl.: *JETP Letters* **2**, 197 (1965)].

<sup>6</sup>R. N. Il'in, V. A. Oparin, F. S. Solov'ev, and N. V. Fedorenko, *Zh. Tekh. Fiz.* **36**, 1241 (1966) [English transl.: *Soviet Phys. - Tech. Phys.* **11**, 921 (1967)].

<sup>7</sup>V. A. Oparin, R. N. Il'in, and E. S. Solov'ev, *Zh. Eksperim. i Teor. Fiz.* **52**, 369 (1967) [English transl.: *Soviet Phys. - JETP* **25**, 240 (1967)].

<sup>8</sup>J. R. Hiskes, Lawrence Radiation Laboratory Report No. UCRL-71422, 1968 (unpublished).

<sup>9</sup>A. H. Futch, Jr., and K. G. Moses, in *Abstracts of the Contributed Papers, of the Fifth International Conference on the Physics of Electronic and Atomic Collisions, 1967* (Nauka, Leningrad, 1968), p. 12; also Lawrence Radiation Laboratory Report No. UCRL-70251 Summary, 1967 (unpublished).

<sup>10</sup>A. C. Riviere, in *Abstracts of the Contributed Papers, of the Fifth International Conference on the Physics of Electronic and Atomic Collisions 1967* (Nauka, Leningrad, 1968), p. 15; also UKAEA Culham Laboratory Progress Report No. CLM-PR 11, 1968, p. B.23 (unpublished).

<sup>11</sup>J. L. Philpot and R. H. Hughes, *Phys. Rev.* **133** A107 (1964).

<sup>12</sup>M. Dufay, J. Desesquelles, M. Druetta, and M. Eidelsberg, *Ann. Géophys.* **22**, 614 (1966).

<sup>13</sup>J. M. Robinson and H. B. Gilbody, *Proc. Phys. Soc. (London)* **92**, 589 (1967).

<sup>14</sup>E. W. Thomas, G. D. Bent, and J. L. Edwards, *Phys. Rev.* **165**, 32 (1968).

<sup>15</sup>The cross section for excitation of the 3914 Å band by H atoms is approximately 30% less than that for H<sup>+</sup> excitation at this energy (Refs. 13 and 16); for the pressures used the atomic fraction of the beam is less than 5%.

<sup>16</sup>D. A. Dahlberg, D. K. Anderson, and I. E. Dayton, *Phys. Rev.* **164**, 20 (1967).

<sup>17</sup>See, for example, E. W. McDaniel, *Collision Phenomena in Ionized Gases* (John Wiley & Sons, Inc., New York, 1964), p. 297.

<sup>18</sup>We justify this by the following argument: We assume that the states of all higher quantum levels  $n''$  are statistically populated and that the relative populations of these levels are proportional to  $n^{-3}$ . Using statistically

weighted transition probabilities  $A(n'' \rightarrow 6)$ , we find the contribution from  $n''=7$  to 11 to be 1.4% of the population of  $n=6$  for the worst case (3.5-cm flight path at 5 keV).

<sup>19</sup>J. R. Hiskes and C. B. Tarter, Lawrence Radiation Laboratory Report No. UCRL-7088 Rev. I, 1964 (unpublished). These authors compared their calculated dipole matrix elements with earlier tabulations (Ref. 20) and found agreement to six significant figures.

<sup>20</sup>L. C. Green, P. P. Rush, and C. D. Chandler, *Astrophys. J. Suppl., Ser. No. 26*, **3**, 37 (1957).

<sup>21</sup>H. A. Bethe and E. E. Salpeter, *Quantum Mechanics of One- and Two-Electron Atoms* (Academic Press, Inc., New York, 1957), Chap. III.

<sup>22</sup>Some other attempts to investigate the assumption of a statistical distribution, or remarks on the possibility of Stark mixing of substates, can be found, e.g., in Refs. 23 to 26. However, we have not been able to find any information that aids in the present analysis.

<sup>23</sup>A. C. Riviere and H. Wind, in UKAEA Culham Laboratory Progress Report No. CLM-PR 7, 1964, p. 48 (unpublished).

<sup>24</sup>R. H. Hughes, H. R. Dawson, and B. M. Doughty, *Phys. Rev.* **164**, 166 (1967).

<sup>25</sup>V. A. Ankudinov, S. V. Bobashev, and E. P. Andreev, *Zh. Eksperim. i Teor. Fiz.* **48**, 40 (1965) [English transl.: *Soviet Phys. - JETP* **21**, 26 (1965)].

<sup>26</sup>E. P. Andreev, V. A. Ankudinov, S. V. Bobashev, and V. B. Matveev, *Zh. Eksperim. i Teor. Fiz.* **52**, 357 (1967) [English transl.: *Soviet Phys. - JETP* **25**, 232 (1967)].

<sup>27</sup>In the Brinkman-Kramers form of the first Born approximation only the interaction of the incoming proton with the target electrons is considered; in the Jackson-Schiff form the interaction of the incoming proton with the target electrons and the target nucleus is considered.

<sup>28</sup>R. A. Mapleton, *Phys. Rev.* **126**, 1477 (1962).

<sup>29</sup>R. A. Mapleton, *J. Phys. B* **1**, 529 (1968).

<sup>30</sup>V. S. Nikolaev, *Zh. Eksperim. i Teor. Fiz.* **51**, 1264 (1966) [English transl.: *Soviet Phys. - JETP* **24**, 847 (1967)].

<sup>31</sup>E. Clementi, *IBM J. Res. Develop.* **9**, 2 (1965) and supplement.

<sup>32</sup>J. R. Hiskes, Lawrence Radiation Laboratory, Livermore, Calif., private communication.

<sup>33</sup>J. C. Slater, *Phys. Rev.* **36**, 57 (1930).

<sup>34</sup>R. A. Mapleton, Air Force Cambridge Research Laboratories, Bedford, Mass., private communication.

<sup>35</sup>R. M. May, *Phys. Rev.* **136**, A669 (1964).

<sup>36</sup>R. A. Mapleton, Air Force Cambridge Research Laboratories Report No. AFCRL-67-0351 (unpublished); *Physical Sciences Research Papers*, No. 328, 1967 (unpublished), pp. 79, 161-166.

<sup>37</sup>To evaluate this ratio we have used the total electron-capture cross sections  $\sigma_{10}$  reported in Ref. 1.

<sup>38</sup>Hiskes's calculations (Refs. 8 and 32) indicate that in the energy range considered here most of the electrons are captured into the  $n=2$  and 3 levels. We therefore define the "effective ground state" to be that cluster of levels of small  $n$  into which most of the electron capture occurs.

<sup>39</sup>A. C. Riviere, Atomic Energy Research Establishment, Harwell, Berkshire, U.K. Report No. AERE-R-4818, 1964 (unpublished), pp. 124-135.

<sup>40</sup>K. H. Berkner, L. Kay, and A. C. Riviere, Nucl. Fusion **7**, 29 (1967).

<sup>41</sup>It has been pointed out by Butler and May [S. T. Butler and R. M. May, Phys. Rev. **137**, A10 (1965)] that ionization of a highly excited level by collisions with atoms should be independent of  $n$ .

<sup>42</sup>P. M. Stier and C. F. Barnett, Phys. Rev. **103**, 896 (1956).

<sup>43</sup>S. V. Bobashev, V. A. Ankudinov, and E. P. Andreev, Zh. Eksperim. i Teor. Fiz. **48**, 833 (1965) [English transl.: Soviet Phys. - JETP **21**, 554 (1965)].

<sup>44</sup>The ordering is obtained from G. Lüders, Ann. Physik **8**, 301 (1951). The method of presenting the ordering follows that used for the  $n=7$  level by A. C. Riviere, Culham Report No. CLM-M23, 1963 (unpublished), Fig. 5.

## Measurement of the Total Cross Section for Charge Transfer into the Metastable State H(2s) for Protons Incident on H<sub>2</sub> and Ar Gases\*

James E. Bayfield

Gibbs Laboratory, Yale University, New Haven, Connecticut 06520

(Received 17 February 1969)

The energy dependence of the total cross section for  $H^+ + H_2 \rightarrow H(2s) + H_2^+$  exhibits two broad maxima in the range 2-70 keV. The lower maximum occurs at an energy where the total charge-transfer cross section is largest, and thus may be due to coupling with the ground-state scattering channel. The observed energy dependence is similar to that for  $H^+ + H_2 \rightarrow Ly \alpha$ , but with the positions of both maxima shifted to higher energies by about 5 keV. The cross section for  $H^+ + Ar \rightarrow H(2s) + Ar^+$  over the extended energy range 2-70 keV also exhibits only two maxima. Internal and external quenching measurements of this cross section are in agreement. Its absolute magnitude at 20 keV has now been independently measured by three investigators, with results consistent with  $\pm 20\%$ .

### I. INTRODUCTION

The measurement of atomic collision cross sections basically involves the determination of three quantities: The incident beam intensity, the thickness of the scattering target, and the scattered beam intensity. In the study of the electron or charge transfer process  $H^+ + X \rightarrow H + X^+$  at keV energies, fast hydrogen atoms produced in the scattering can be separated from elastically scattered protons by an electric or magnetic deflection field. The study of charge transfer into an excited state  $H(nl)$  necessitates additional state-sensitive detection of a portion of the scattered atom beam.

The metastable H(2s) atom component of a fast hydrogen-atom beam can be selectively detected through induced decay. An external dc electric field applied to the beam couples the long-lived 2s state with the nearby short-lived 2p state. At sufficiently high fields the mixed state has a short lifetime and decays to the ground state within the field region. This Stark-effect quenching of meta-

stable atoms therefore results in the emission of Lyman-alpha ( $Ly-\alpha$ ) photons; an intensity measurement of this radiation determines the intensity of the metastable atom beam.

The direct study of charge transfer into H(2s) was first undertaken by Madansky and Owen<sup>1</sup> using a 10-keV proton beam and an H<sub>2</sub> gas-scattering target. It was known that charge transfer would occur at relatively large impact parameters, and that atomic scattering at keV energies is approximately controlled by the screened Coulomb potential. Thus an "external-quenching" type of experiment was performed, in which fast H(2s) atoms were searched for outside the scattering cell, within a small solid angle centered around the direction of the incident beam. This experimental approach to measuring the cross section  $\sigma_{2s}(H_2)$  for the  $H^+ + H_2$  system has been used by several investigators studying differing energy ranges.<sup>2-4</sup>

Measurements of  $\sigma_{2s}$  have also been made for protons incident on inert-gas targets.<sup>5-7</sup> Argon scattering targets were used by Jaecks, Van Zyl,